Soil Advances 2 (2024) 100017

Contents lists available at ScienceDirect

Soil Advances

journal homepage: www.sciencedirect.com/journal/soil-advances

Exploring carbon storage and sequestration as affected by land use/land cover changes toward achieving sustainable development goals

Bahman Veisi Nabikandi [a], Farzin Shahbazi [b,*], Ahmad Hami [a], Brendan Malone [c]

[a] Landscape Architecture Department, Faculty of Agriculture, University of Tabriz, 5166616471, Iran
[b] Soil Science Department, Faculty of Agriculture, University of Tabriz, 5166616471, Iran
[c] CSIRO Agriculture and Food, Bruce E. Butler Laboratory, PO Box 1700, Canberra, ACT 2601, Australia

ARTICLE INFO

Keywords:
Azarshahr city
carbon pools
CA-Markov model
InVEST model
LULC changes
sustainable development goals

ABSTRACT

Understanding the impact of changes in land use/land cover (LULC) on carbon sequestration (C_{seq}) and emission leads to achieving sustainable development goals (SDGs). For this, Business-As-Usual (BAU) and Sustainable Development (SD) scenarios were examined in Azarshar city, Iran which is faced with urban intensification. The spatiotemporal dynamics of the carbon cycle and influences of various urban growth indicators are still unclear even under climate change, rapid urbanization, and ecological deterioration. In this research, total carbon storage (C_{ts}) and C_{seq} were determined at four carbon pools i.e., aboveground carbon (AGC), belowground carbon (BGC), dead organic carbon (DeOC), and soil organic carbon (SOC). This research revealed a successful implementation of integrated CA-Markov and InVEST models in delineating LULC changes between 2013 and 2033. It was concluded that land resources management play a crucial role in decreasing C_{seq} along with increasing carbon emission across the study area. The modelling results showed a significant shifting from barren and cropland to developed land uses. This research goes beyond providing supporting evidence that urban expansion is a key factor driving the aforementioned changes, but also illustrates the importance of remote sensing in ecological modelling, especially where information is sparse.

1. Introduction

Over the last decades, land use/land cover (LULC) changes especially due to urban intensification has increased (Yuan et al., 2022). LULC changes are important metrics in assessing progress toward sustainable development goals (SDGs) (Guo et al., 2023). Wei et al. (2023) elucidated the impact of rapid urbanization in China's urban land use on diminishing SDGs. There are 17 interlinked goals defined by the United Nations SDGs. Since there was a lack of SDG-oriented evaluation of urban land use at a local level, it would be of interest to monitor total carbon storage (C_{ts}) and carbon sequestration (C_{seq}) following LULC changes. The literature demonstrates that landscape changes and accelerated urbanization throughout the world– including Iran, particularly in metropolitan areas in recent decades– have led to widespread changes in the spatial pattern of the landscape (Dadashpoor et al., 2019). According to the Human Development Report issued by the United Nations, the urbanization rate in Iran was 64.20 % in 2000, then increased to 75.94 % in 2019, and it was expected to increase to 85.82 % by 2050 (Pilehvar, 2021). Therefore, among the SDGs, the 15th being: Sustainably manage forests, combat desertification, halt and reverse land degradation, halt biodiversity loss; can be measured in places like Azarshahr city, located in north-western Iran due to significant growth in anthropogenic activities this city has faced in recent decades.

The expansion of urbanization leads to increased carbon emission due to declining ecological spaces in the environment (Wu et al., 2023). Furthermore, carbon emissions due to anthropogenic activities, i.e., using fossil fuels, deforestation, and undesirable land use changes, contribute to global warming (Lu et al., 2022). Consequently, carbon

Abbreviations: LULC, Land Use/Land Cover; SDGs, Sustainable development goals; C_{ts}, Total carbon storage; C_{seq}, Carbon sequestration; IPCC, Intergovernmental Panel on Climate Change; RS, Remote sensing; DSM, Digital soil mapping; BAU, Business-As-Usual; SD, Sustainable Development; CA-Markov, Cellular Automata-Markov; InVEST, Integrated Valuation of Ecosystem Services and Tradeoffs; AGC, Aboveground carbon; BGC, Belowground carbon; DeOC, Dead organic carbon; SOC, Soil organic carbon; DEM, Digital elevation model; GIS, Geographic information system; USGS, United States Geological Survey; SVM, Support vector machine; CA, Cellular Automata; SOCS, Soil Organic Carbon Storage.

* Corresponding author.
E-mail address: shahbazi@tabrizu.ac.ir (F. Shahbazi).

https://doi.org/10.1016/j.soilad.2024.100017
Received 24 June 2024; Received in revised form 24 August 2024; Accepted 24 August 2024
Available online 31 August 2024

emissions due to fossil energy consumption, as well as its role in climate change, will be of significant concern (Qin and Sha, 2023). Moreover, C_{seq} can be mentioned as one of the most important crises affected by climate change (Gallant et al., 2020). The Intergovernmental Panel on Climate Change (IPCC) has facilitated the provision of useful information for policymakers to address both present and potential future risks (Masson-Delmotte et al., 2022).

LULC changes impact the spatiotemporal patterns of carbon emission and C_{seq} (Hong et al., 2022). Decreasing carbon emissions and increasing C_{seq} are crucial parameters to achieve SDGs in urban areas (Hong et al., 2023). The segregation of urban areas from other land use scenarios, i.e., agriculture, forest, pasture, and water body sectors also explain their spatial distribution (Castella et al., 2013). Overall, urbanization accelerates natural resource vulnerability, increasing impervious surfaces and reducing green spaces (Santhanam and Majumdar, 2022). Many nations and regions have transformed substantial tracts of forest, croplands, and pasture into industrial zones to intensify economic prosperity. Therefore, a significant amount of the available carbon pool has transformed into a carbon source (Le Bivic and Melot, 2020; Yang et al., 2020). To address this, monitoring the spatiotemporal patterns of environmental features needs to be modeled and mapped with the application of easy-to-measure attributes, i.e., remote sensing (RS) data (Shahbazi et al., 2019) and advanced methods. For example, RS data has been incorporated into digital soil mapping (DSM) projects, providing highly detailed characterization of soil resources and their functions (Mulder et al., 2011). Moreover, the time series of LULC changes can be demonstrated using RS data derived from Landsat imagery and calculated band ratios (Piao et al., 2021).

The simulation of LULC changes at various scenarios i.e., business-as-usual (BAU) as a baseline and sustainable development (SD) assists in identifying C_{ts} and C_{seq} for different carbon pools. For this, the Cellular Automata-Markov (CA-Markov) model has been consistently used with confident results (Koko et al., 2020). Basse et al. (2014) found that CA-Markov would be a useful tool for generating a geographic pattern for landscape with transition principles. A similar finding had been reported by Yang et al. (2012). The next user-friendly model in ecological monitoring is the Integrated Valuation of Ecosystem Services and Tradeoffs (InVEST) to assess and simulate the carbon cycle in terrestrial

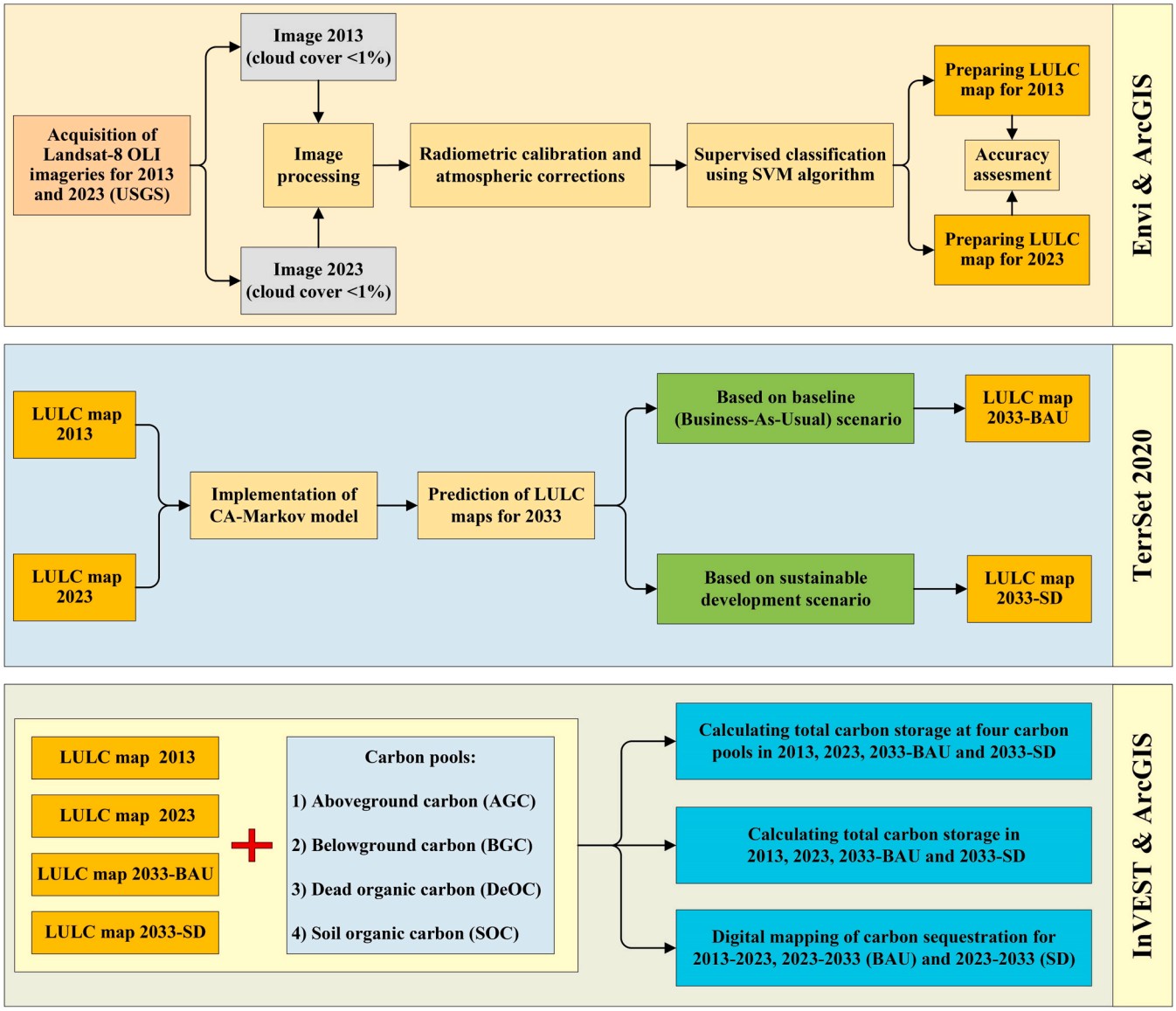

Fig. 1. The flowchart of the methodology used in this research. USGS: United States Geological Survey; SVM: Support Vector Machine; LULC: Land use/land cover; CA-Markov: Cellular Automata-Markov Chain; BAU: Business-As-Usual; SD: Sustainable Development; InVEST: Integrated Valuation of Ecosystem Services and Tradeoffs.

ecosystems (Kafy et al., 2023). It evaluates sequestered carbon among different pools i.e., soil, plants, and other sources over considerable time scales (Gallant et al., 2020). Furthermore, integrating CA-Markov and InVEST models have been frequently used in environmental modelling i.e., prediction of C_{seq} both in Iran (Sadat et al., 2020) and the world (He et al., 2016; Babbar et al., 2021). Additionally, Clerici et al. (2019) found the aforementioned models' ability to assess the combined consequences of LULC and increased temperatures on the services in the Colombian Andes.

Since urban intensification is one of the most important drivers of climate change (Li et al., 2022a), a set of software i.e., TerrSet, Envi, and InVEST in addition to ArcGIS were utilized in this study. Therefore, our research aimed: i) to distinguish the LULC changes using RS data derived from Landsat-8 OLI (Operational Land Imager) imagery acquired for 2013 and 2023; ii) to predict the LULC changes for 2033 using Markov chain method based on two scenarios of BAU and SD and to compare the results; iii) to calculate C_{seq} for the next decade according to the above-mentioned scenarios; and iv) to observe C_{ts} and C_{seq} as a result of LULC changes at four carbon pools i.e., aboveground carbon (AGC), belowground carbon (BGC), dead organic carbon (DeOC) and soil organic carbon (SOC).

2. Materials and methods

2.1. Simplified flowchart of the study

Fig. 1 shows the flowchart of the methodology implemented in this research to ease the visualization of the process. The first step was to prepare LULC maps for 2013 and 2023 using available RS data. Subsequently, these were utilized in preparing LULC maps for 2033 based on the two defined scenarios, i.e., BAU and SD. The amount of C_{ts} for the four carbon pools and then C_{seq} over the study area based on the LULC maps were also calculated.

2.2. Study area and general description

This research was conducted in Azarshahr city with an areal extent of about 173.70 km^2. It is located in East Azerbaijan Province, Iran. It is delimited by longitude 45°50′42″ - 46°02′11″ E and latitude 37°43′16″ - 37°52′37″ N (Fig. 2-a and b). The digital elevation model (DEM) of the study area indicates that altitude varies from 1270 to 1557 m above sea level with an increasing trend from the western to the eastern part of the study area (Fig. 2-c). According to the report of the IRIMO (2020) for the last 15 consecutive years, the average annual maximum and minimum temperatures are 27.7 °C and 3.7 °C (15.25 °C, on average), respectively. The annual rainfall and evapotranspiration on average are 303 mm and 1500 mm, respectively. According to the Keys to Soil Taxonomy (USDA, 2014) and the clipped study site from the original soil map of Iran at

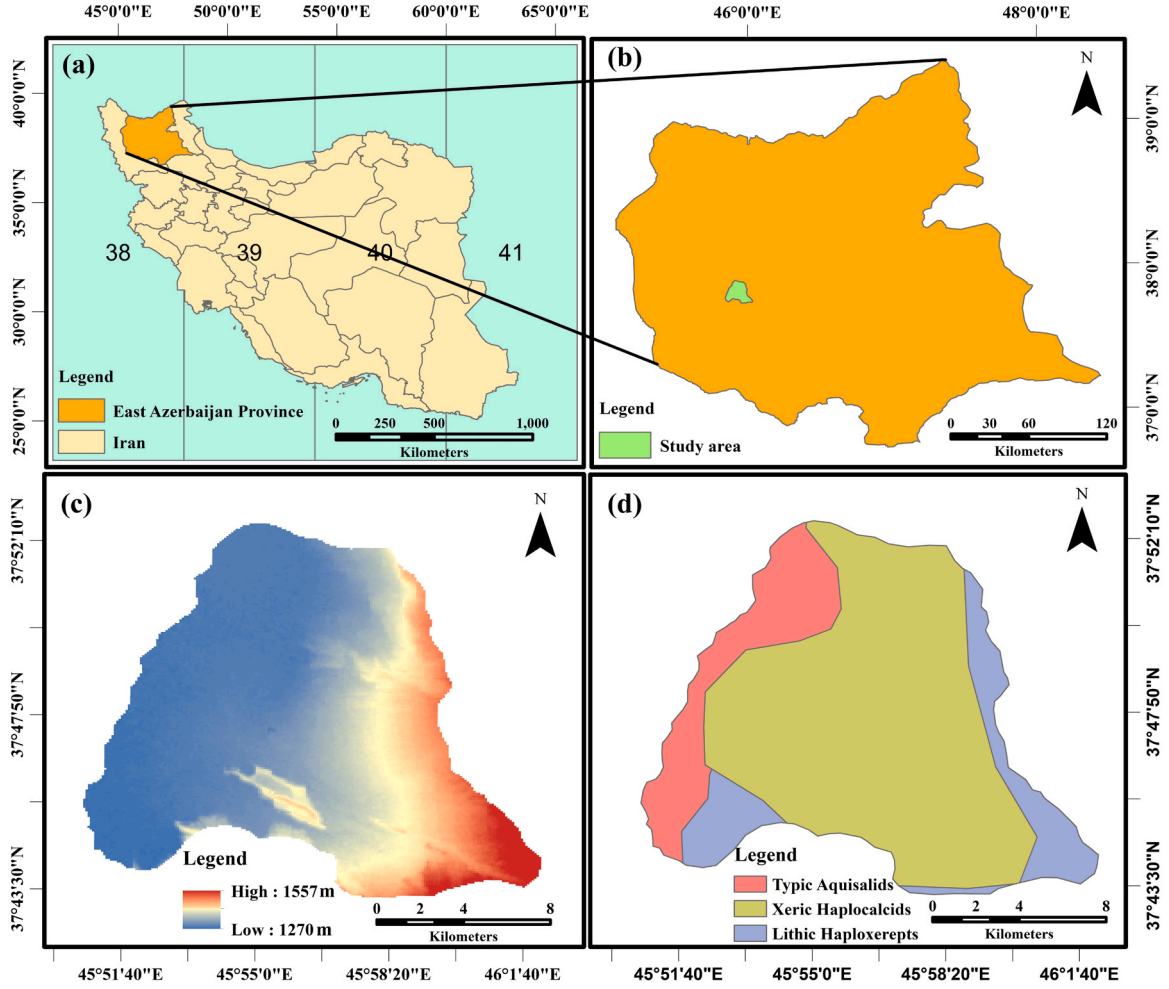

Fig. 2. Location of the study area in Iran (a) and in East Azerbaijan Province (b); digital elevation model (DEM) for the entire study area (c), and identified three soil subgroups across the study area (d).

1:1000,000 scale, three soil subgroups were identified. The dominant soil subgroups are Xeric Haplocalcids (70 %), followed by Typic Aquisalids (16 %) and Lithic Haploxerepts (14 %) (Fig. 2-d).

2.3. Remotely-sensed data

The simultaneous implementation of RS data and geographic information system (GIS) facilitates preparing LULC maps. Primarily, those are needed for calculating C_{ts} values for each land use (Babbar et al., 2021). This research acquired Landsat-8 OLI satellite data for July 2013 and June 2023 (via USGS-EROS; http://earthexplorer.usgs.gov/). For both scenes, RS data pre-processing i.e., radiometric calibration and atmospheric correction were performed (Poncet et al., 2019; Doxani et al., 2023). A major reason for selecting the above-mentioned data capture dates was due to the ideal condition of zero cloud coverage. While the native resolution of the RS scenes was 30-m pixel resolution, we resampled whole images to 15-m resolution in order to improve LULC classification (Phiri et al., 2018) through clearer characterization of the plant cover and bare soil in the examined region (El Haj et al., 2023).

2.4. Preparing LULC maps

The acquired RS data were used in preparing LULC maps for 2013 and 2023. For this, the support vector machine (SVM) algorithm was used in supervised classification mode. Although, it is a powerful supervised algorithm that makes use of a binary classifier founded in statistical machine learning theory (Vapnik, 1998), we used SVM in classifying the entire study area into six classes i.e., developed, cropland, tree cover (scrub forest), pasture, barren, and water body based on the known Land Cover Class categorizations (USGS, 2022). The high accuracy of the results when using SVM in land cover classification has been reported by Asori and Adu (2023).

2.4.1. Accuracy of prepared maps

To evaluate the accuracy of supervised classification, the kappa statistic criterion was used in this research. Yilmaz and Demirhan (2023) reported that kappa is a good indicator for evaluating multi-class classification performance. After classifying LULC changes, a total of 236 points (both in 2013 and 2023) were randomly selected according to their available coordinates covering six examined LULC classes across the study area. Due to the variation of area extension relevant to each class, the number of selected points differed for each. Each random point's value was then verified using Google Earth for accuracy assessment. Similar work has been performed by Tilahun and Teferie (2015) to verify Google Earth's ability to segregate various land uses i.e., agriculture, settlement, grazing, forest, and bare lands in addition to water bodies in Ethiopia.

2.4.2. Prediction of LULC maps for 2033

To monitor the LULC changes and to prepare their maps to describe SDGs, two scenarios were defined by the fact that scenario analysis through the creation of alternative plans and policies is an effective approach to assess ecosystem services i.e., C_{ts} due to land use changes (Wang et al., 2022b). These were Business-As-Usual (BAU) versus Sustainable Development (SD). BAU refers to a hypothetical situation in which the current conditions, trends, policies, or operations of a system or a process remain unchanged or unaffected by any significant change or intervention, often used as a standard or a benchmark for comparing and evaluating impacts. SD on the other hand, is a hypothetical situation in which the current or future land use and environmental policies are designed to prioritize ecological conservation and restoration over economic development to achieve SDGs (Gaur and Singh, 2023). One expects to observe clear differences and non-aligned trajectories between the aforementioned scenarios. For the SD scenario, tree cover and grasslands were prohibited from being converted to agricultural and built-up areas, and urban growth and development are controlled and regulated to improve management and decision-making (Dougaheh et al., 2023). At this step, the LULC maps for 2033 were prepared based on BAU and SD scenarios. For this, the following approaches were consecutively performed:

2.4.2.1. Markov chain. The Markov chain model within the TerrSet software was utilized in this study for geospatial monitoring and modelling since it simultaneously incorporates image processing tools for sustainable development purposes (Eastman, 2016). Since Markov chain specifically focuses on spatial transformation without accounting for influencing factors (Sun et al., 2022), it was used by tabulating the relative frequency of change for all transitions between the six studied land uses. Using land cover data for the 2013 and 2023, the probability of a transition in LULC for year 2033 were calculated for the two aforementioned scenarios. Obviously, in the studies related to land resources, the shifts between different land use categories may vary or remain somewhat constant over time. Therefore, the actual transition probability matrix was employed to predict future land use changes based on historical data for each land use category (Ghalehteimouri et al., 2022). Regarding identified changes of LULC for the last 10 years era (from 2013 to 2023) using Markov chain, the modelling processes were pursued using Cellular Automata (CA).

2.4.2.2. Cellular automata model. The CA model was then used as a mathematical framework to illustrate the area of LULC changes over time. It generates self-similar patterns and uniform states (Wolfram, 1983) which represent cellular actions, reactions, and quantified variations in each cell's attributes based on a set of pre-defined rules. CA has been commonly utilized to simulate LULC changes. Notwithstanding the CA model assisting in finding the evolving patterns of urban growth (Wang and Maduako, 2018), it is ideally suited for integration with other models due to its dynamic and temporal nature (Ghalehteimouri et al., 2022). Therefore, CA was linked with Markov chain in this study to observe the LULC changes from 2013 to 2023.

2.4.2.3. CA-Markov model. One of the prominent models commonly used for predicting upcoming LULC is the combination of CA and Markov chain, referred to as the CA-Markov model (Song et al., 2020; Negese et al., 2022). According to the distinguished LULC changes based on the aforementioned models' outputs for the past time periods, we implemented the CA-Markov model within the TerrSet software to prepare the LULC map for 2033-BAU and 2033-SD. Obviously, it was expected to observe urban expansion (developed) due to increasing population and needs to support food and living requirements, and on the contrary, decreasing of cropland, tree cover, pasture, barren and water body areas. The ability of CA-Markov model in urban planning and land suitability assessment across the globe was reported by Mishra et al. (2018). The LULC changes impact on temperature over the study area and greenhouse gases (Nayak and Mandal, 2019), therefore, monitoring the C_{seq} would be of interest, which can be evaluated by InVEST model.

2.5. InVEST model for calculating carbon sequestration

To directly calculate soil organic carbon storage (SOCS) in the field, abundant data derived from laboratory analyses and digital soil mapping (DSM) techniques are essential (Rahbar Alam Shirazi et al., 2023). Soil analyses incur siginifican costs, both in monetary and time investments, therefore, linking CA-Markov and InVEST model facilitates the representing of static C_{ts} and temporal C_{seq} within a landscape (Zhao et al., 2019). The carbon pools i.e., AGC, BGC, DeOC and SOC were calculated using InVEST model based on the available LULC maps (Leh et al., 2013; Babbar et al., 2021). Carbon storage data for each pool can be sourced from field estimates obtained through local design studies,

extracted from meta-analyses focusing on specific habitat types or regions, or derived from established scientific literature. For reference, these are summarized in Table 1.

Although, different procedures were examined and there was no literature and background related to our study area, we used carbon density data (on average) focusing on the previous findings i.e. (Ma et al., 2019; Sadat et al., 2020; Li et al., 2021a; Adelisardou et al., 2022; Wang et al., 2022a). Furthermore, Clerici et al. (2019) found that due to representation of the data from a single time point, researchers can ignore the effects of LUCC on carbon storage changes. A possible clarification for averaging is that initial data extracted from the literature were somewhat similar to our study area in terms of latitude. A decisive reason is that latitude affects the humus decomposition rate as well as SOC accumulation (Li et al., 2022b). It should be noted that the results may be changed if the input data such as the application of IPCC guidelines (IPCC, 2006) or InVEST user's guide (Sharp et al., 2020) are supplied.

The InVEST model calculates the C_{ts} per unit area at six LULC using Eqs.1 and 2, respectively.

$$C = AGC + BGC + DeOC + SOC \quad (1)$$

$$C_{ts} = \sum_{k=1}^{n} A_k \times C_{k,} (k = 1, \quad 2, \quad \ldots n) \quad (2)$$

where, C represents the summation of calculated carbon density at four pools interrelated to each LULC in Mg ha^{-1}. Subsequently, by multiplying the average carbon density of the aforementioned pools along with each LULC (C_k) in their respective areas (A_k), the amount of C_{ts} was computed in Mg (Zhao et al., 2019; Hu et al., 2021). The next step was to utilize the prepared digital maps of C_{ts} for 2013, 2023 and 2033 (BAU and SD scenarios) for calculating C_{seq} for the aforementioned three-time scenarios. Finally, in addition to illustrating the variation of C_{seq} from 2013 to 2023, it was presented for the future (2023–2033) by implementing two scenarios (BAU and SD).

3. Results and discussion

3.1. Retrospective monitoring of LULC changes

3.1.1. Final LULC maps

The LULC maps for 2013, 2023 and based on future projection for 2033 in terms of examined BAU and SD scenarios are illustrated in Fig. 3.

The built model for 2013 relevant to our study area showed that the highest area was covered by croplands (33.8 %), followed by barren (24.8 %), pasture (19.3 %), developed (12.7 %), tree cover (9.3 %) and water body (0.1 %). The developed land use and water bodies are predominantly located in the lower elevation areas with gentle slopes. Furthermore, tree cover was concentrated toward the central part of the study area. A similar procedure was performed in preparation of LULC map for 2023. The visualization of using predicted maps for 2033 show a distinct variation on land uses by time.

Table 1
The used carbon density (Mg ha^{-1}) in InVEST model.

LULC classes	AGC	BGC	DeOC	SOC
Developed	0.10	0.00	0.00	14.77
Cropland	3.62	2.61	0.50	34.24
Tree Cover	29.67	7.95	3.28	26.34
Pasture	1.64	3.28	0.07	62.48
Barren	0.61	0.47	0.00	7.70
Water body	0.84	5.98	0.00	6.25

AGC: aboveground carbon; BGC: belowground carbon; DeOC: dead organic carbon; SOC: soil organic carbon.

3.1.2. LULC change analyses

Fig. 4 illustrates the decadal analysis of LULC changes from 2013 till now and for the future. In terms of 2013–2033, the highest variation was for pasture (-11 %), followed by developed (+10 %), barren (+8.6 %), cropland (-4.1 %) and tree cover (-3.6 %) land uses. Since there was no detectable change in terms of water body, it was ignored in the analysis process. It should be noted that the classification accuracy for 2013 and 2023 based on the kappa coefficient values was 0.82 and 0.81, respectively (Table 2).

According to the Markov chain model for the year between 2013 and 2023, a significant change was identified in the central part of the study area with the conversion of 743 ha of barren to developed land uses. Additionally, 905 ha of cropland was converted to development over the examined period. The Markov chain indicates the likelihood of moving from one state to another as a stochastic process where conditions within a system shift from one state to another with defined transition probabilities (Fogang et al., 2023). The results provide supporting evidence that urban expansion is likely attributed to this area. This urbanization was previously reported in China (Wang et al., 2023), India (Mishra et al., 2020) and even in Iran (Sobhani et al., 2021). Moreover, 872 ha of cropland and 1718 ha of pasture have been converted to barren land in the same period.

In terms of future projections, the BAU scenario shows an increase of 7.6 % in developed while a decrease of 4.4 %, 1.7 %, 0.6 % and 0.9 % area extension in cropland, tree cover, pasture and barren, respectively. While, SD scenario shows a decrease in area extension in cropland (-8.1 %) and increase of 1.7 %, 4.8 % and 1.6 % for tree cover, pasture and barren, respectively. The most frequently observed changes from 2023 to 2033 under BAU scenario were for barren to developed (822 ha), followed by croplands to developed (474 ha) and croplands to barren (458 ha). The next examined scenario (SD) for 2023–2033 demonstrated the conversion of 891 ha croplands to barren, 288 ha cropland to tree cover and 225 ha cropland to pasture. Obviously, these conversions result in an improvement of ecological spaces across the study area.

3.2. Total carbon storage

The next step was to calculate C_{ts} across the study area based on the prepared LULC maps for 2013 and 2023 as well as the predicted one for 2033 (BAU and SD scenarios) through linking CA-Markov and InVEST models. This procedure has previously been implemented in similar disciplines (Hernández-Guzmán et al., 2019; Hoque et al., 2021; Zhu et al., 2022; Adelisardou et al., 2022). However, the calculation of C_{ts} at four carbon pools i.e., AGC, BGC, DeOC and SOC in past, present and future has not been well investigated. Fig. 5 presents the results of the integrated modelling for each of the carbon pools. Fig. 6 illustrates the spatial distribution of C_{ts} in Mg ha^{-1} for the entire study area.

3.2.1. Past to present era

According to the results, the highest carbon storage was considered for SOC, followed by AGC, BGC and DeOC at all examined time scenarios. In 2013, the highest levels of C_{ts} relate to SOC (80.3 %), followed by AGC (12 %), BGC (6.4 %) and DeOC (1.3 %). A similar trend was also observed for 2023 (SOC=81.6 %, AGC=11.2 %, BGC=6 % and DeOC=1.2 %). Gong et al. (2022) found similar results in China; our study area in terms of climate and landscape is somewhat similar to Nandu River Basin on Hainan Island. Since SOC was distinguished as having the highest levels of C_{ts} in all scenarios, it may be explained by urbanization as well as increasing barren land in our study area. Obviously, it depends on the circumstances of the study area. For instance, Barakat et al. (2021) elucidated that urbanization associated with population growth and economic development significantly affected LULC change and tended to reduce the area of agricultural fields and then SOC deposition. In summary, a total of 160,823 Mg C_{ts} (approximately 25 %) decreased from 2013 to 2023 (Supplementary material, Table A1). The

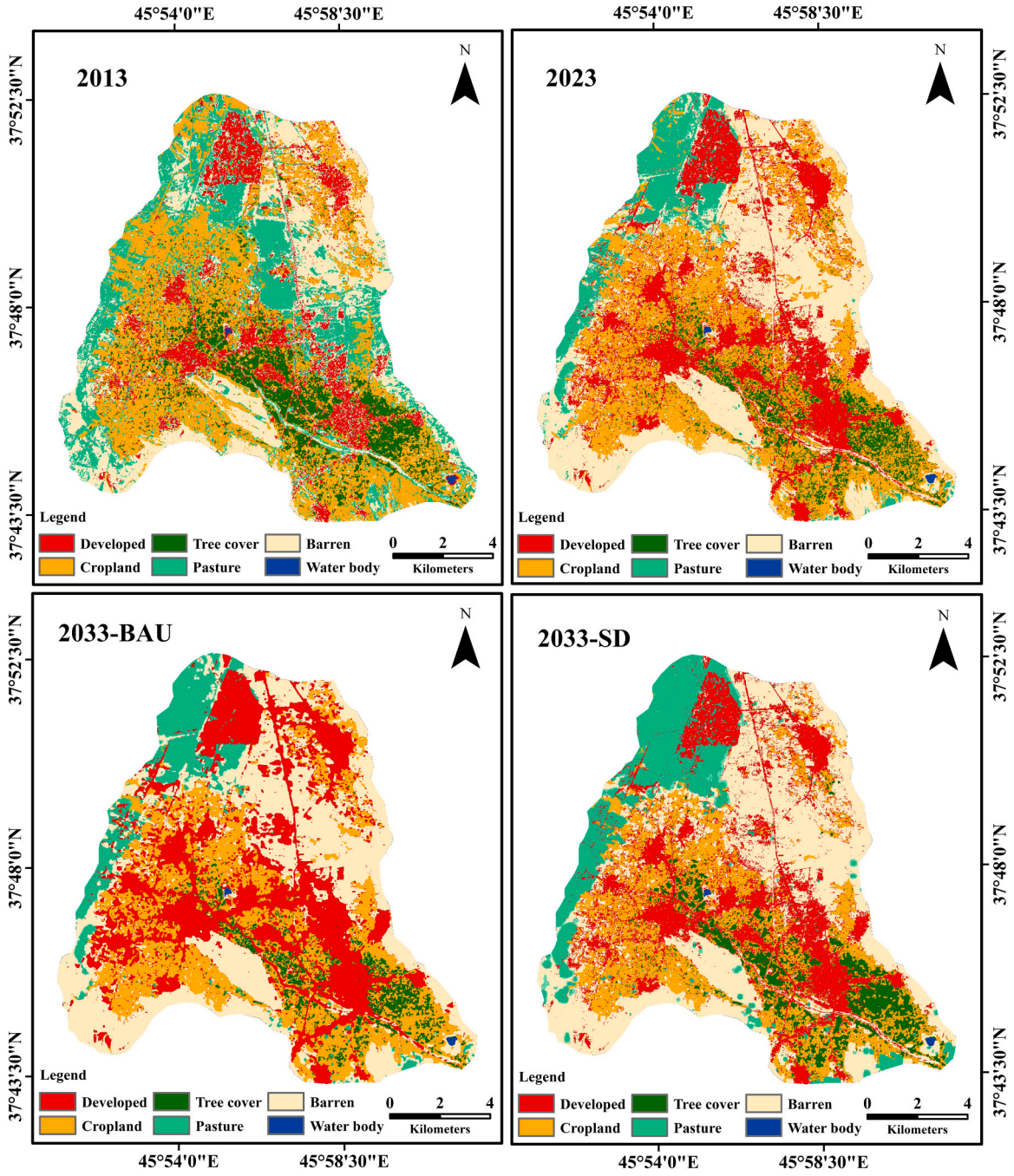

Fig. 3. Prepared LULC maps for the entire study area in 2013 and 2023 as well as predicted ones in 2033 based on scenarios of BAU and SD.

results reveal that C_{ts} has a 1.33-fold decrease in variation between their values in 2013 and 2023. A similar declining trend due to urbanization was observed in Shanghai, China (Zhang et al., 2020), represented by 73.19×10^5 Mg C_{ts} (0.48 % per year) from 1990–2015. On the contrary, Li et al. (2021a) reported that there was an increase of 11.8 % C_{ts} in 2016 compared to 2000. Details in terms of the calculated C_{ts} at examined carbon pools and LULC in 2013, 2023 as well as 2033 (BAU and SD scenarios) are summarized in Supplementary material, Table A1.

3.2.2. *Future scenario analysis*

In terms of future scenario analysis (2023–2033), the C_{ts} based on BAU showed a somewhat similar decreasing trend (by 39,750 Mg) from past to present as expected (4-fold). A possible reason is that the study area has no more potential for urban intensification. A complementary regular decreasing trend was also observed at four carbon pools because LULC changes directly threaten carbon storage (Jiang et al., 2017). The highest levels of C_{ts} for SOC (83.9 %), followed by AGC (9.6 %), BGC (5.4 %) and DeOC (1.1 %). Therefore, a 1.08-fold declining variation between 2023 and 2033-BAU indicates a decreased rate of C_{ts} accumulation in the next 10 years. Obviously, the rate of C_{seq} impacts on carbon emission. Goldstein et al. (2020) confirmed the huge effects of urban land expansion on C_{ts} followed by carbon emission.

The second scenario, SD, revealed an increment of 21,140 Mg C_{ts} for the entire study area. The difference among two examined scenarios can be explained by the fact that SD results were taken after controlling urban development and protecting ecological spaces. The highest value was found for SOC (81 %), followed by AGC (11.8 %), BGC (6 %) and DeOC (1.2 %). In summary, the C_{ts} increased by 12 % when using SD

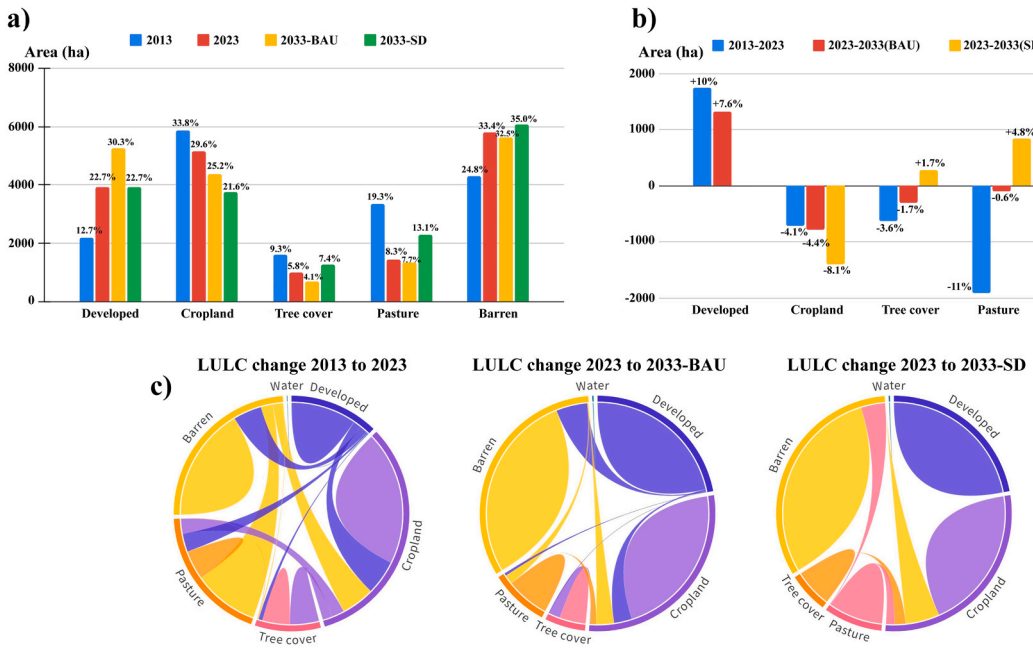

Fig. 4. The decadal analysis and future projections (a and b) along with Chord diagram (c) indicating LULC changes for the past and future eras (BAU and SD scenarios).

Table 2
The classification accuracy of different LULC classes using evaluating criteria.

Year	LULC Class	Validation points for different LULC classes							
		Developed	Cropland	Tree Cover	Pasture	Barren	Water body	**Total**	**User Accuracy**
2013	Developed	40	0	0	0	3	0	43	93.02
	Cropland	0	31	0	2	4	0	37	83.78
	Tree Cover	0	3	45	0	0	0	48	93.75
	Pasture	2	2	0	40	4	0	48	83.33
	Barren	3	0	0	10	37	0	50	74.00
	Water body	0	0	0	0	0	10	10	100.00
	Total	45	36	45	52	48	10	236	
	Producer Accuracy	88.89	86.11	100.00	76.92	77.08	100.00	Overall Accuracy 86.01 %	Kappa Coefficient 0.82
2023	Developed	45	3	0	2	1	0	51	88.24
	Cropland	1	41	5	0	3	0	50	82.00
	Tree Cover	0	4	28	0	1	0	33	84.85
	Pasture	2	0	0	35	3	0	40	87.50
	Barren	2	3	0	6	41	0	52	78.85
	Water body	0	0	0	0	0	10	10	100.00
	Total	50	51	33	43	49	10	236	
	Producer Accuracy	90.00	80.39	84.85	81.40	83.67	100.00	Overall Accuracy 84.74 %	Kappa Coefficient 0.81

LULC: Land use/land cover

compared to BAU. This can be explained by the increase of tree cover and pasture land uses which is parallel on achieving UN SDGs. Zhang et al. (2023) found that an environmental protection scenario has the greatest impact on achieving SDG15.1 in coastal urban areas. Kafy et al. (2023) reported the influence of land management practices i.e., afforestation, reforestation, and conservation agriculture on the amount of C_{ts}. Generally, this study highlighted the importance of policy and land management interventions in enhancing C_{ts} which primarily needed for explaining C_{seq} (Critchley et al., 2023). A brief description of stored carbon under BAU and SD scenarios are summarized in Supplementary material (Table A1).

3.3. Carbon sequestration

Understanding C_{seq} following the calculation of C_{ts} is important because human activities i.e., LULC changes have far-reaching consequences for CO_2 emission (Sha et al., 2022). The first direct demonstration of this research was the enablement of monitoring the spatial distribution of C_{seq} by LULC changes using RS data and modelling techniques. Contrary to field measurements and digital mapping of C_{seq} through environmental covariates (Siami et al., 2022), our approach is cost- and time-efficient. Fig. 7 shows the spatial distribution of sequestered carbon and carbon emission across the study area over the period 2013–2023 as well as for the future based on two examined scenarios.

The maps were categorized into three classes to facilitate the interpretations. The results revealed that in 2013–2023, the highest carbon emission occurs in the central part of the study area because this area faced extensive changes of coverage and there is a net decrease in carbon. Generally, a total of 31.6 % of the study area emits more carbon than they absorb. However, the CO_2 emissions caused by LULC changes are possibly larger than assumed (Arneth et al., 2017). Further observation illustrates an increasing area expansion of no-change in future. Consequently, it demonstrates a stabilization of land use patterns, which could be attributed to policy interventions or natural succession processes (Lambin and Meyfroidt, 2010).

The details of C_{seq} values related to the examined pools are briefly

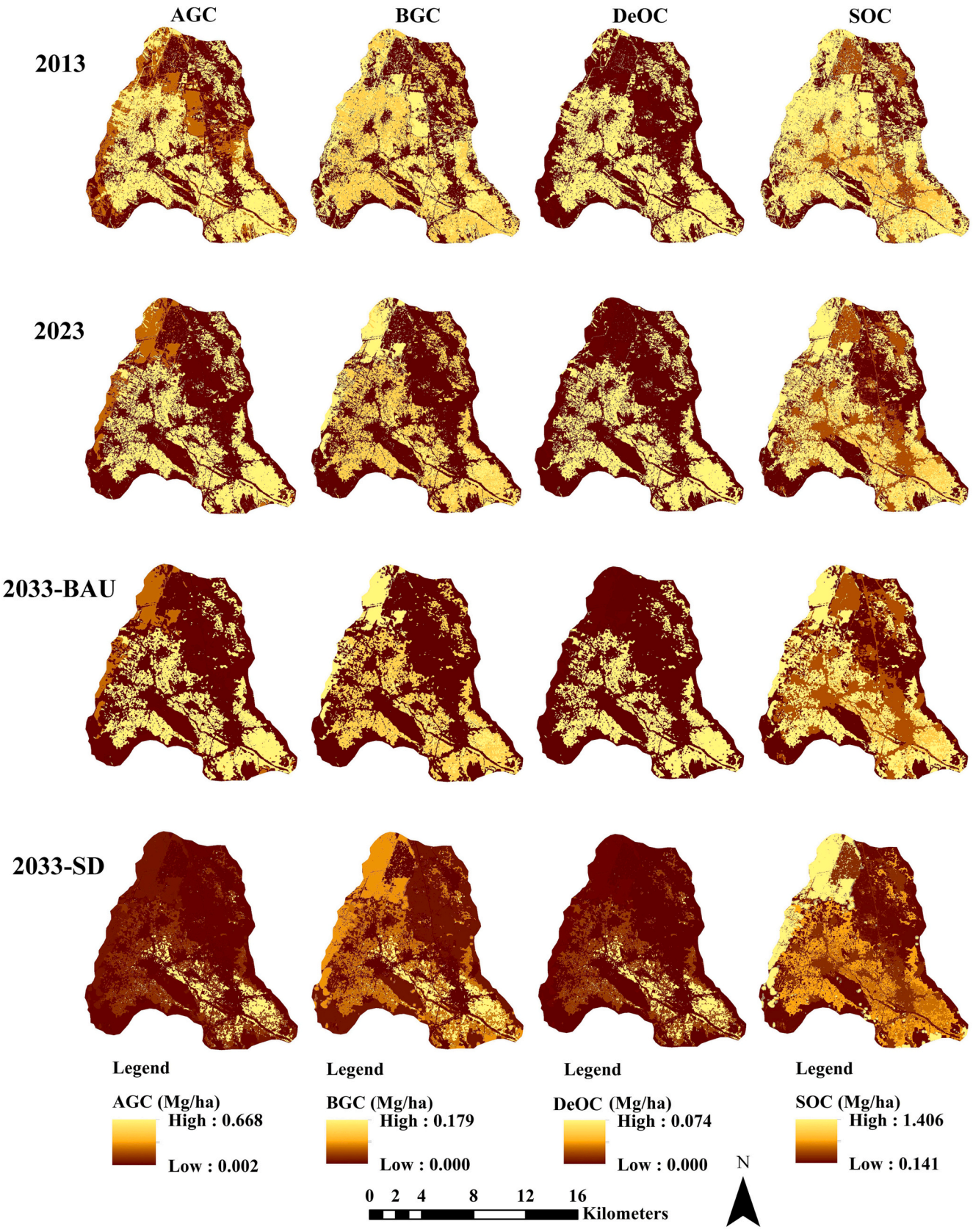

Fig. 5. The spatiotemporal distribution of total carbon storage considering for each carbon pool across the study area.

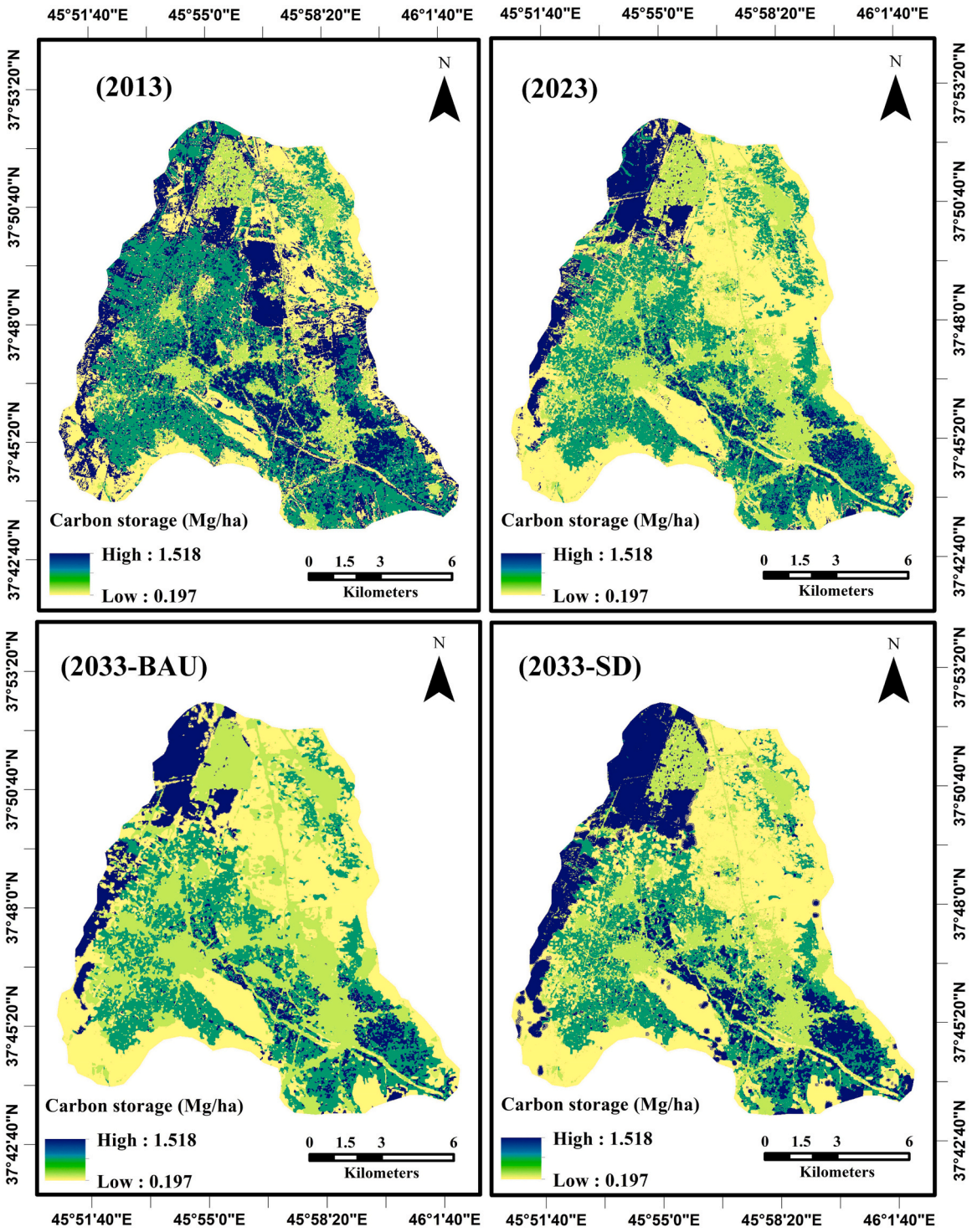

Fig. 6. The spatial distribution of total carbon storage for the entire study area in past, present and future time eras.

described in Supplementary material, Table A2. The negative values of C_{seq} demonstrate carbon emissions. The results show an emission of 160,823 Mg carbon from 2013 to 2023. This finding strongly implies that barren lands were increasingly converted to pasture from 2013 to 2023. In terms of future projection, notwithstanding there was no more C_{seq} difference between BAU and SD, while both scenarios demonstrated that C_{seq} would be decreased by 2-fold (6.5 %-6.6 %) compared to 2023. Taken together, our finding indicates differences in carbon emission values among BAU and SD scenarios, representing 9.1 % and 5.3 %, respectively. One possible interpretation is that under SD scenario, the positive impact of targeted environmental policies and land management strategies were mentioned (Cao et al., 2023). Land resources management i.e., agricultural practices and urbanization were the most important factors in decreasing C_{seq} along with increasing carbon emission across the study area by the fact that SOCS is a key function of soils as affected by LULC changes (Wiesmeier et al., 2019).

Finally, our findings not only imply a dynamic interplay between aforementioned carbon pools over time, but it can also be concluded that land use changes across the study area had a negative impact on carbon reservoirs (Betts, 2000). Furthermore, the continuous degradation of the

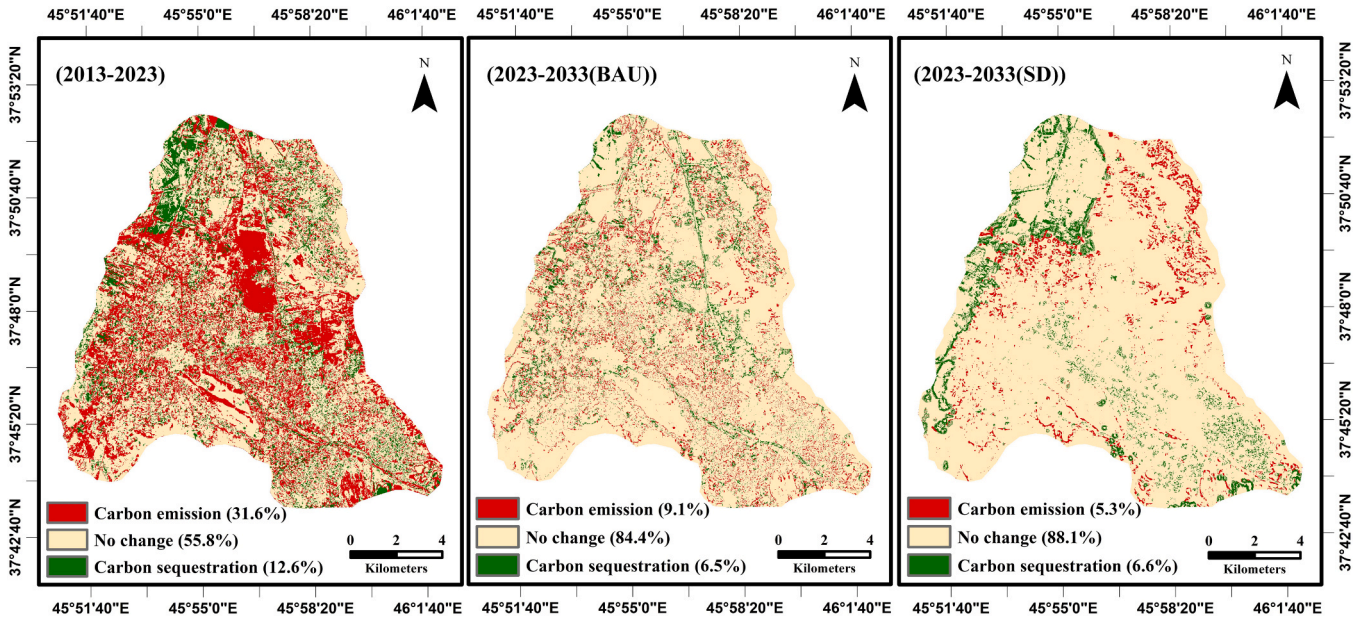

Fig. 7. Spatial distribution of carbon sequestration and emission across the study area during the period 2013–2023 and 2023–2033 (BAU and SD scenarios).

environment because of rapid economic growth and urbanization has contributed to the issue of global warming (Chen et al., 2022). We also obtained evidence that our study area is faced with C_{seq} and emission over time.

3.4. Study limitations and future directions

The present research provided clear support for classification and prediction of LULC maps for Azarshahr city in past, present and future scenarios. One basic potential limitation with this research is the absence of high-resolution RS data (e.g., Li et al., 2021b) and satellite hyperspectral image (Meng et al., 2021) for 2013. An accurate result may be taken when using other RS data. For instance, Velazquez et al. (2022) revealed the successful mapping of SOC using integrated indices as a novel idea in the Mediterranean area (Spain). The next limitation is the lack of soil legacy data and field measurements for our study site. Moreover, the limited availability of specific literature for Iran in calculating the AGC, BGC, DeOC, and SOC coefficients would be another limitation. Despite these limitations, an average of carbon density was utilized in InVEST model based on previous works from around the world with some similarity to our study area (Ma et al., 2019; Li et al., 2021a; Wang et al., 2022a). Therefore, complementary work is needed to fill the gaps between ecological modelling and monitoring the impacts of LULC changes on C_{seq} in Azarshahr. Additionally, the findings may raise a variety of intriguing questions for future study, and this can be considered to be the most important contribution. With a lack of LULC changes, information over the study area and even over Iran, this study would represent a low-cost framework to track LULC changes across the county, province and then throughout the country.

4. Conclusion

This study comprehensively analyses the spatiotemporal dynamics of carbon storage and C_{seq} in Azarshahr city by linking CA-Markov and InVEST models using available RS data. It also gives a direct pathway to calculating C_{seq} by aggregating stored carbon from different carbon pools i.e., AGC, BGC, DeOC and SOC using prepared LULC changes maps with the absence of field data.

According to the results, carbon content over 2013–2023 has decreased dramatically and stands to decrease at a slower rate from 2023 to the predicted year of 2033. Urban intensification was identified as the main factor in reducing C_{seq} across the study area. Furthermore, a significant reduction in C_{seq} capacity was found due to the loss of environmental ecological spaces, i.e., tree covers, pastures, and agriculture. To overcome this, effective land use management strategies are indispensable to minimize the environmental impacts of human activities on C_{seq} capacity.

This research emphasizes the important role of RS in monitoring LULC changes in short- and long-term scenarios. Linking CA-Markov and InVEST models as an innovative approach assisted us in monitoring the spatiotemporal analyses of C_{ts} and C_{seq} based on LULC changes. Finally, our research reveals a deeper understanding of the links between LULC induced by environmental restoration programs and carbon storage changes. It is concluded that some practices i.e., afforestation and reforestation programs as well as encouraging tourism development, can reduce the adverse effects of LULC changes on C_{seq}.

CRediT authorship contribution statement

Bahman Veisi Nabikandi: Writing – review & editing, Writing – original draft, Software, Methodology, Investigation, Formal analysis, Data curation, Conceptualization. **Farzin Shahbazi:** Writing – review & editing, Supervision, Project administration, Methodology, Investigation, Data curation, Conceptualization. **Ahmad Hami:** Supervision, Investigation, Data curation. **Brendan Malone:** Writing – review & editing.

Declaration of Competing Interest

The authors declare that they have no known competing financial interests or personal relationships that could have appeared to influence the work reported in this paper.

Data Availability

Data will be made available on request.

Acknowledgment

This research did not receive any specific grant from funding agencies in the public, commercial, or not-for-profit sectors. The authors also express heartfully appreciations from the anonymous reviewers and

editor in advance.

Appendix A. Supporting information

Supplementary data associated with this article can be found in the online version at doi:10.1016/j.soilad.2024.100017.

References

Adelisardou, F., Zhao, W., Chow, R., Mederly, P., Minkina, T., Schou, J.S., 2022. Spatiotemporal change detection of carbon storage and sequestration in an arid ecosystem by integrating Google Earth Engine and InVEST (the Jiroft plain, Iran). Int. J. Environ. Sci. Technol. 19, 5929–5944. https://doi.org/10.1007/s13762-021-03676-6.

Arneth, A., Sitch, S., Pongratz, J., Stocker, B.D., Ciais, P., Poulter, B., Bayer, A.D., Bondeau, A., Calle, L., Chini, L.P., Gasser, T., Fader, M., Friedlingstein, P., Kato, A., Li, W., Lindeskog, M., Nabel, J.E.M.S., Pugh, T.A.M., Robertson, E., Viovy, N., Yue, C., Zaehle, S., 2017. Historical carbon dioxide emissions caused by land-use changes are possibly larger than assumed. Nat. Geosci. 10, 79–84. https://doi.org/10.1038/ngeo2882.

Asori, M., Adu, P., 2023. Modelling the impact of the future state of land use land cover change patterns on land surface temperatures beyond the frontiers of greater Kumasi: A coupled cellular automaton (CA) and Markov chains approaches. Remote Sens. Appl.: Soc. Environ. 29, e100908 https://doi.org/10.1016/j.rsase.2022.100908.

Babbar, D., Areendran, G., Sahana, M., Sarma, K., Raj, K., Sivadas, A., 2021. Assessment and prediction of carbon sequestration using Markov chain and InVEST model in Sariska Tiger Reserve, India. J. Clean. Prod. 278, e123333 https://doi.org/10.1016/j.jclepro.2020.123333.

Barakat, A., Khellouk, R., Touhami, F., 2021. Detection of urban LULC changes and its effect on soil organic carbon stocks: a case study of Béni Mellal City (Morocco). J. Sediment. Environ. 6, 287–299. https://doi.org/10.1007/s43217-020-00047-y.

Basse, R.M., Omrani, H., Charif, O., Gerber, P., Bódis, K., 2014. Land use changes modelling using advanced methods: cellular automata and artificial neural networks. The spatial and explicit representation of land cover dynamics at the cross-border region scale. Appl. Geogr. 53, 160–171. https://doi.org/10.1016/j.apgeog.2014.06.016.

Betts, R.A., 2000. Offset of the potential carbon sink from boreal forestation by decreases in surface albedo. Nature 408, 187–190. https://doi.org/10.1038/35041545.

Cao, M., Tian, Y., Wu, K., Chen, M., Chen, Y., Hu, X., Sun, Z., Zuo, L., Lin, J., Luo, L., Zhu, R., Xu, Z., Bandrova, T., Konecny, M., Yuan, W., Guo, H., Lin, H., Lü, G., 2023. Future land-use change and its impact on terrestrial ecosystem carbon pool evolution along the Silk Road under SDG scenarios. Sci. Bull. 68, 740–749. https://doi.org/10.1016/j.scib.2023.03.012.

Castella, J.C., Lestrelin, G., Hett, C., Bourgoin, J., Fitriana, Y.R., Heinimann, A., Pfund, J. L., 2013. Effects of landscape segregation on livelihood vulnerability: moving from extensive shifting cultivation to rotational agriculture and natural forests in northern Laos. Hum. Ecol. 41, 63–76. https://doi.org/10.1007/s10745-012-9538-8.

Chen, F., Liu, A., Lu, X., Zhe, R., Tong, J., Akram, R., 2022. Evaluation of the effects of urbanization on carbon emissions: the transformative role of government effectiveness. Front. Energy Res. 10, e848800 https://doi.org/10.3389/fenrg.2022.848800.

Clerici, N., Cote-Navarro, F., Escobedo, F.J., Rubiano, K., Villegas, J.C., 2019. Spatio-temporal and cumulative effects of land use-land cover and climate change on two ecosystem services in the Colombian Andes. Sci. Total Environ. 685, 1181–1192. https://doi.org/10.1016/j.scitotenv.2019.06.275.

Critchley, W., Harari, N., Mollee, E., Mekdaschi-Studer, R., Eichenberger, J., 2023. Sustainable land management and climate change adaptation for small-scale land users in sub-Saharan Africa. Land 12, 1206. https://doi.org/10.3390/land12061206.

Dadashpoor, H., Azizi, P., Moghadasi, M., 2019. Land use change, urbanization, and change in landscape pattern in a metropolitan area. Sci. Total Environ. 655, 707–719. https://doi.org/10.1016/j.scitotenv.2018.11.267.

Dougaheh, M.P., Ashofteh, P.S., Loáiciga, H.A., 2023. Urban stormwater management using low-impact development control measures considering climate change. Theor. Appl. Climatol. 154, 1021–1033. https://doi.org/10.1007/s00704-023-04604-z.

Doxani, G., Vermote, E.F., Roger, J.C., Skakun, S., Gascon, F., Collison, A., De Keukelaere, L., Desjardins, C., Frantz, D., Hagolle, O., Kim, M., Louis, J., Pacifici, F., Pflug, B., Poilvé, H., Ramon, D., Richter, R., Yin, F., 2023. Atmospheric Correction Inter-comparison eXercise, ACIX-II land: an assessment of atmospheric correction processors for Landsat 8 and Sentinel-2 over land. Remote Sens. Environ. 285, e113412 https://doi.org/10.1016/j.rse.2022.113412.

Eastman, J.R., 2016. TerrSet Geospatial Monitoring and Modelling System. Clark University: Worcester, MA, USA, pp. 345–389.

El Haj, F.A., Ouadif, L., Akhssas, A., 2023. Simulating and predicting future land-use/land cover trends using CA-Markov and LCM models. Case Stud. Chem. Environ. Eng. 7, e100342 https://doi.org/10.1016/j.cscee.2023.100342.

Fogang, L.F., Tiomo, I.F., Kamga, B.Y., Kpoumie, H.M., Nkondjoua, A.D.T., Nguetsop, V. F., Zapfack, L., 2023. Predicting land use/land cover changes in the Santchou Wildlife Reserve (Santchou, West-Cameroon) using a CA-Markov model. Trees, For. People 151, e100438. https://doi.org/10.1016/j.tfp.2023.100438.

Gallant, K., Withey, P., Risk, D., van Kooten, G.C., Spafford, L., 2020. Measurement and economic valuation of carbon sequestration in Nova Scotian wetlands. Ecol. Econ. 171, e106619 https://doi.org/10.1016/j.ecolecon.2020.106619.

Gaur, S., Singh, R., 2023. A comprehensive review on land use/land cover (LULC) change modeling for urban development: current status and future prospects. Sustainability 15, 903. https://doi.org/10.3390/su15020903.

Ghalehteimouri, K.J., Shamsoddini, A., Mousavi, M.N., Ros, F.B.C., Khedmatzadeh, A., 2022. Predicting spatial and decadal of land use and land cover change using integrated cellular automata Markov chain model based scenarios (2019–2049) Zarriné-Rūd River Basin in Iran. Environ. Chall. 6, e100399 https://doi.org/10.1016/j.envc.2021.100399.

Goldstein, A., Turner, W.R., Spawn, S.A., Anderson-Teixeira, K.J., Cook-Patton, S., Fargione, J., Gibbs, H.K., Griscom, B., Hewson, J.H., Howard, J.F., Ledezma, J.C., Page, S., Koh, L.P., Rockström, J., Sanderman, J., Hole, D.G., 2020. Protecting irrecoverable carbon in Earth's ecosystems. Nat. Clim. Change 10, 287–295. https://doi.org/10.1038/s41558-020-0738-8.

Gong, W., Duan, X., Mao, M., Hu, J., Sun, Y., Wu, G., Zhang, Y., Xie, Y., Qiu, X., Rao, X., Liu, T., Liu, T., 2022. Assessing the impact of land use and changes in land cover related to carbon storage by linking trajectory analysis and InVEST models in the Nandu River Basin on Hainan Island in China. Front. Environ. Sci. 10, e1038752 https://doi.org/10.3389/fenvs.2022.1038752.

Guo, H., Chen, F., Tang, Y., Ding, Y., Chen, M., Zhou, W., Zhu, M., Gao, S., Yang, R., Zheng, W., Fang, C., Lin, H., Roders, A.P., Cigna, F., Tapete, D., Xu, B., 2023. Progress toward the sustainable development of world cultural heritage sites facing land-cover changes. Innovation 4, e100496. https://doi.org/10.1016/j.xinn.2023.100496.

He, C., Zhang, D., Huang, Q., Zhao, Y., 2016. Assessing the potential impacts of urban expansion on regional carbon storage by linking the LUSD-urban and InVEST models. Environ. Model. Softw. 75, 44–58. https://doi.org/10.1016/j.envsoft.2015.09.015.

Hernández-Guzmán, R., Ruiz-Luna, A., González, C., 2019. Assessing and modeling the impact of land use and changes in land cover related to carbon storage in a western basin in Mexico. Remote Sens. Appl.: Soc. Environ. 13, 318–327. https://doi.org/10.1016/j.rsase.2018.12.005.

Hong, C., Zhao, H., Qin, Y., Burney, J.A., Pongratz, J., Hartung, K., Moore, F.C., Jackson, R.B., Zhang, Q., Davis, S.J., 2022. Land-use emissions embodied in international trade. Science 376, 597–603. https://doi.org/10.1126/science.abj1572.

Hong, G., Tan, C., Qin, L., Wu, X., 2023. Identification of priority areas for UGI optimisation under carbon neutrality targets: perspectives from China. Ecol. Indic. 148, e110045 https://doi.org/10.1016/j.ecolind.2023.110045.

Hoque, M.Z., Cui, S., Islam, I., Xu, L., Ding, S., 2021. Dynamics of plantation forest development and ecosystem carbon storage change in coastal Bangladesh. Ecol. Indic. 130, e107954 https://doi.org/10.1016/j.ecolind.2021.107954.

Hu, X., Li, Z., Chen, J., Nie, X., Liu, J., Wang, L., Ning, K., 2021. Carbon sequestration benefits of the grain for Green Program in the hilly red soil region of southern China. Int. Soil Water Conserv. Res. 9, 271–278. https://doi.org/10.1016/j.iswcr.2020.11.005.

IPCC, 2006. Intergovernmental Panel on Climate Change. Guidelines for National Greenhouse Gas Inventories. http://www.ipcc-nggip.iges.or.jp/public/2006gl/index.Htm.

IRIMO, 2020. Islamic Republic of Iran Meteorological Organization. Tehran, Iran.

Jiang, W., Deng, Y., Tang, Z., Lei, X., Chen, Z., 2017. Modelling the potential impacts of urban ecosystem changes on carbon storage under different scenarios by linking the CLUE-S and the InVEST models. Ecol. Model. 345, 30–40. https://doi.org/10.1016/j.ecolmodel.2016.12.002.

Kafy, A.A., Saha, M., Fattah, M.A., Rahman, M.T., Duti, B.M., Rahaman, Z.A., Arpita, B., Kalaivani, S., Rahaman, S.N., Sattar, G.S., 2023. Integrating forest cover change and carbon storage dynamics: leveraging Google Earth Engine and InVEST model to inform conservation in hilly regions. Ecol. Indic. 152, e110374 https://doi.org/10.1016/j.ecolind.2023.110374.

Koko, A.F., Yue, W., Abubakar, G.A., Hamed, R., Alabsi, A.A.N., 2020. Monitoring and predicting spatio-temporal land use/land cover changes in Zaria City, Nigeria, through an integrated cellular automata and markov chain model (CA-Markov). Sustainability 12, e10452. https://doi.org/10.3390/su122410452.

Lambin, E.F., Meyfroidt, P., 2010. Land use transitions: Socio-ecological feedback versus socio-economic change. Land Use Policy 27, 108–118. https://doi.org/10.1016/j.landusepol.2009.09.003.

Le Bivic, C., Melot, R., 2020. Scheduling urbanization in rural municipalities: local practices in land-use planning on the fringes of the Paris region. Land Use Policy 99, e105040. https://doi.org/10.1016/j.landusepol.2020.105040.

Leh, M.D., Matlock, M.D., Cummings, E.C., Nalley, L.L., 2013. Quantifying and mapping multiple ecosystem services change in West Africa. Agric., Ecosyst. Environ. 165, 6–18. https://doi.org/10.1016/j.agee.2012.12.001.

Li, G., Fang, C., Li, Y., Wang, Z., Sun, S., He, S., Qi, W., Bao, C., Ma, H., Fan, Y., Feng, Y., Liu, X., 2022a. Global impacts of future urban expansion on terrestrial vertebrate diversity. Nat. Commun. 13, e1628 https://doi.org/10.1038/s41467-022-29324-2.

Li, X., Yang, T., Hicks, L.C., Hu, B., Liu, X., Wei, D., Wang, Z., Bao, W., 2022b. Latitudinal patterns of light and heavy organic matter fractions in arid and semi-arid soils. Catena 215, e106293. https://doi.org/10.1016/j.catena.2022.106293.

Li, K., Cao, J., Adamowski, J.F., Biswas, A., Zhou, J., Liu, Y., Zhang, Y., Liu, C., Dong, X., Qin, Y., 2021a. Assessing the effects of ecological engineering on spatiotemporal dynamics of carbon storage from 2000 to 2016 in the Loess Plateau area using the InVEST model: a case study in Huining County, China. Environ. Dev. 39, e100641 https://doi.org/10.1016/j.envdev.2021.100641.

Li, Y., Zhao, Z., Wei, S., Sun, D., Yang, Q., Ding, X., 2021b. Prediction of regional forest soil nutrients based on Gaofen-1 remote sensing data. Forests 12, e1430. https://doi.org/10.3390/f12111430.

Lu, Z.Q., Wu, C.G., Wu, N.Y., Lu, H.L., Wang, T., Xiao, R., Liu, H., Wu, X.H., 2022. Change trend of natural gas hydrates in permafrost on the Qinghai-Tibet Plateau (1960–2050) under the background of global warming and their impacts on carbon emissions. China Geol. 5, 475–509. https://doi.org/10.31035/cg2022034.

Ma, T., Li, X., Bai, J., Ding, S., Zhou, F., Cui, B., 2019. Four decades' dynamics of coastal blue carbon storage driven by land use/land cover transformation under natural and anthropogenic processes in the Yellow River Delta, China. Sci. Total Environ. 655, 741–750. https://doi.org/10.1016/j.scitotenv.2018.11.287.

Masson-Delmotte, V., Zhai, P., Pörtner, H.O., Roberts, D., Skea, J., Shukla, P.R., 2022. Global Warming of 1.5° C: IPCC Special Report on Impacts of Global Warming of 1.5° C above Pre-industrial Levels in Context of Strengthening Response to Climate Change, Sustainable Development, and Efforts to Eradicate Poverty. Cambridge University Press. https://doi.org/10.1017/9781009157940.

Meng, X., Bao, Y., Ye, Q., Liu, H., Zhang, X., Tang, H., Zhang, X., 2021. Soil organic matter prediction model with satellite hyperspectral image based on optimized denoising method. Remote Sens. 13, 2273. https://doi.org/10.3390/rs13122273.

Mishra, P.K., Rai, A., Rai, S.C., 2020. Land use and land cover change detection using geospatial techniques in the Sikkim Himalaya, India. Egypt. J. Remote Sens. Space Sci. 23, 133–143. https://doi.org/10.1016/j.ejrs.2019.02.001.

Mishra, V.N., Rai, P.K., Prasad, R., Punia, M., Nistor, M.M., 2018. Prediction of spatio-temporal land use/land cover dynamics in rapidly developing Varanasi district of Uttar Pradesh, India, using geospatial approach: a comparison of hybrid models. Appl. Geomat. 10, 257–276. https://doi.org/10.1007/s12518-018-0223-5.

Mulder, V.L., De Bruin, S., Schaepman, M.E., Mayr, T.R., 2011. The use of remote sensing in soil and terrain mapping—a review. Geoderma 162, 1–19. https://doi.org/10.1016/j.geoderma.2010.12.018.

Nayak, S., Mandal, M., 2019. Impact of land use and land cover changes on temperature trends over India. Land Use Policy 89, e104238. https://doi.org/10.1016/j.landusepol.2019.104238.

Negese, A., Worku, D., Shitaye, A., Getnet, H., 2022. Potential flood-prone area identification and mapping using GIS-based multi-criteria decision-making and analytical hierarchy process in Dega Damot district, northwestern Ethiopia. Appl. Water Sci. 12, 255. https://doi.org/10.1007/s13201-022-01772-7.

Phiri, D., Morgenroth, J., Xu, C., Hermosilla, T., 2018. Effects of pre-processing methods on Landsat OLI-8 land cover classification using OBIA and random forests classifier. Int. J. Appl. Earth Obs. Geoinf. 73, 170–178. https://doi.org/10.1016/j.jag.2018.06.014.

Piao, Y., Jeong, S., Park, S., Lee, D., 2021. Analysis of land use and land cover change using time-series data and random forest in North Korea. Remote Sens. 13, 3501. https://doi.org/10.3390/rs13173501.

Pilehvar, A.A., 2021. Spatial-geographical analysis of urbanization in Iran. Humanit. Soc. Sci. Commun. 8, 63. https://doi.org/10.1057/s41599-021-00741-w.

Poncet, A.M., Knappenberger, T., Brodbeck, C., Fogle Jr, M., Shaw, J.N., Ortiz, B.V., 2019. Multispectral UAS data accuracy for different radiometric calibration methods. Remote Sens. 11, 1917. https://doi.org/10.3390/rs11161917.

Qin, Z., Sha, Z., 2023. Modelling the impact of urbanization and climate changes on terrestrial vegetation productivity in China by a neighborhood substitution analysis. Ecol. Model. 482, e110405 https://doi.org/10.1016/j.ecolmodel.2023.110405.

Rahbar Alam Shirazi, F., Shahbazi, F., Rezaei, H., Biswas, A., 2023. Digital assessments of soil organic carbon storage using digital maps provided by static and dynamic environmental covariates. Soil Use Manag. 39, 948–974. https://doi.org/10.1111/sum.12900.

Sadat, M., Zoghi, M., Malekmohammadi, B., 2020. Spatiotemporal modelling of urban land cover changes and carbon storage ecosystem services: case study in Qaem Shahr County, Iran. Environ., Dev. Sustain. 22, 8135–8158. https://doi.org/10.1007/s10668-019-00565-4.

Santhanam, H., Majumdar, R., 2022. Quantification of green-blue ratios, impervious surface area and pace of urbanisation for sustainable management of urban lake–land zones in India-a case study from Bengaluru city. J. Urban Manag. 11, 310–320. https://doi.org/10.1016/j.jum.2022.03.001.

Sha, Z., Bai, Y., Li, R., Lan, H., Zhang, X., Li, J., Liu, X., Chang, S., Xie, Y., 2022. The global carbon sink potential of terrestrial vegetation can be increased substantially by optimal land management. Commun. Earth Environ. 3, 8. https://doi.org/10.1038/s43247-021-00333-1.

Shahbazi, F., McBratney, A.B., Malone, B.P., Oustan, S., Minasny, B., 2019. Retrospective monitoring of the spatial variability of crystalline iron in soils of the east shore of Urmia Lake, Iran using remotely sensed data and digital maps. Geoderma 337, 1196–1207. https://doi.org/10.1016/j.geoderma.2018.11.024.

Sharp, R., Douglass, J., Wolny, S., Arkema, K., Bernhardt, J., Bierbower, W., Chaumont, N., Denu, D., Fisher, D., Glowinski, K., Griffin, R., Guannel, G., Guerry, A., Johnson, J., Hamel, P., Kennedy, C., Kim, C.K., Lacayo, M., Lonsdorf, E., Mandle, L., Rogers, L., Silver, J., Toft, J., Verutes, G., Vogl, A.L., Wood, S., Wyatt, K., 2020. InVEST 3.8.7., User's Guide. The Natural Capital Project, Standford University, University of Minnesota. The Nature Conservancy, and World Wildlife Fund, Standford, CA, USA.

Siami, A., Aliasgharzad, N., Maleki, L.A., Najafi, N., Shahbazi, F., Biswas, A., 2022. Recalcitrant C source mapping utilizing solely terrain-related attributes and data mining techniques. Agronomy 12, 1653. https://doi.org/10.3390/agronomy12071653.

Sobhani, P., Esmaeilzadeh, H., Mostafavi, H., 2021. Simulation and impact assessment of future land use and land cover changes in two protected areas in Tehran, Iran. Sustain. Cities Soc. 75, e103296 https://doi.org/10.1016/j.scs.2021.103296.

Song, S., Liu, Z., He, C., Lu, W., 2020. Evaluating the effects of urban expansion on natural habitat quality by coupling localized shared socioeconomic pathways and the land use scenario dynamics-urban model. Ecol. Indic. 112, e106071 https://doi.org/10.1016/j.ecolind.2020.106071.

Sun, C., Bao, Y., Vandansambuu, B., Bao, Y., 2022. Simulation and prediction of land use/cover changes based on CLUE-S and CA-Markov models: a case study of a typical pastoral area in Mongolia. Sustainability 14, e15707. https://doi.org/10.3390/su142315707.

Tilahun, A., Teferie, B., 2015. Accuracy assessment of land use land cover classification using Google Earth. Am. J. Environ. Prot. 4, 193–198. https://doi.org/10.11648/j.ajep.20150404.14.

USDA, 2014. Twelfth edition. Keys to Soil Taxonomy. Soil Survey Staff, USA.

USGS, 2022. The United States Geological Survey, Land Cover Class Legend. https://www.usgs.gov/media/images/land-cover-class-legend.

Vapnik, V., 1998. The support vector method of function estimation. NonlineaR Modelling: Advanced Black-box Techniques. Springer US, Boston, MA, pp. 55–85. https://doi.org/10.1007/978-1-4615-5703-6_3.

Velazquez, F.J.B., Shahabi, M., Rezaei, H., González-Peñalozam, F., Shahbazi, F., Anaya-Romero, M., 2022. The possibility of spatial mapping of SOC content at three depths using easy-to-obtain ancillary data in a Mediterranean area. Open Res. Eur. 2, e110 https://doi.org/10.12688/openreseurope.14716.1.

Wang, C., Liu, S., Zhou, S., Zhou, J., Jiang, S., Zhang, Y., Feng, T., Zhang, H., Zhao, Y., Lai, Z., Cui, S., Mao, X., 2023. Spatial-temporal patterns of urban expansion by land use/land cover transfer in China. Ecol. Indic. 155, e111009 https://doi.org/10.1016/j.ecolind.2023.111009.

Wang, J., Maduako, I.N., 2018. Spatio-temporal urban growth dynamics of Lagos Metropolitan Region of Nigeria based on Hybrid methods for LULC modelling and prediction. Eur. J. Remote Sens. 51, 251–265. https://doi.org/10.1080/22797254.2017.1419831.

Wang, N., Chen, X., Zhang, Z., Pang, J., 2022a. Spatiotemporal dynamics and driving factors of county-level carbon storage in the Loess Plateau: a case study in Qingcheng County, China. Ecol. Indic. 144, e109460 https://doi.org/10.1016/j.ecolind.2022.109460.

Wang, Z., Li, X., Mao, Y., Li, L., Wang, X., Lin, Q., 2022b. Dynamic simulation of land use change and assessment of carbon storage based on climate change scenarios at the city level: a case study of Bortala, China. Ecol. Indic. 134, e108499 https://doi.org/10.1016/j.ecolind.2021.108499.

Wei, C., Meng, J., Zhu, L., Han, Z., 2023. Assessing progress towards sustainable development goals for Chinese urban land use: a new cloud model approach. J. Environ. Manag. 326, e116826 https://doi.org/10.1016/j.jenvman.2022.116826.

Wiesmeier, M., Urbanski, L., Hobley, E., Lang, B., von Lützow, M., Marin-Spiotta, E., van Wesemael, B., Rabot, E., Ließ, M., Garcia-Franco, N., Wollschläger, U., Vogel, H., Kögel-Knabner, I., 2019. Soil organic carbon storage as a key function of soils-a review of drivers and indicators at various scales. Geoderma 333, 149–162. https://doi.org/10.1016/j.geoderma.2018.07.026.

Wolfram, S., 1983. Statistical mechanics of cellular automata. Rev. Mod. Phys. 55, 601. https://doi.org/10.1103/RevModPhys.55.601.

Wu, W., Xu, L., Zheng, H., Zhang, X., 2023. How much carbon storage will the ecological space leave in a rapid urbanization area? Scenario analysis from Beijing-Tianjin-Hebei Urban Agglomeration. Resour., Conserv. Recycl. 189, e106774 https://doi.org/10.1016/j.resconrec.2022.106774.

Yang, X., Zheng, X.Q., Lv, L.N., 2012. A spatiotemporal model of land use change based on ant colony optimization, Markov chain and cellular automata. Ecol. Model. 233, 11–19. https://doi.org/10.1016/j.ecolmodel.2012.03.011.

Yang, Y., Bao, W., Li, Y., Wang, Y., Chen, Z., 2020. Land use transition and its eco-environmental effects in the Beijing–Tianjin–Hebei urban agglomeration: a production–living–ecological perspective. Land 9, 285. https://doi.org/10.3390/land9090285.

Yilmaz, A.E., Demirhan, H., 2023. Weighted kappa measures for ordinal multi-class classification performance. Appl. Soft Comput. 134, e110020 https://doi.org/10.1016/j.asoc.2023.110020.

Yuan, J., Lin, Q., Chen, S., Zhao, H., Xie, X., Cai, Z., Zhang, J., Cheng, T., Hua, M., Zhang, R., 2022. Influence of global warming and urbanization on regional climate of Megacity: a case study of Chengdu, China. Urban Clim. 44, e101227 https://doi.org/10.1016/j.uclim.2022.101227.

Zhang, F., Xu, N., Wang, C., Wu, F., Chu, X., 2020. Effects of land use and land cover change on carbon sequestration and adaptive management in Shanghai, China. Phys. Chem. Earth, Parts A/B/C. 120, e102948 https://doi.org/10.1016/j.pce.2020.102948.

Zhang, Z., Jiang, W., Peng, K., Wu, Z., Ling, Z., Li, Z., 2023. Assessment of the impact of wetland changes on carbon storage in coastal urban agglomerations from 1990 to 2035 in support of SDG15. 1. Sci. Total Environ. 877, e162824 https://doi.org/10.1016/j.scitotenv.2023.162824.

Zhao, M., He, Z., Du, J., Chen, L., Lin, P., Fang, S., 2019. Assessing the effects of ecological engineering on carbon storage by linking the CA-Markov and InVEST models. Ecol. Indic. 98, 29–38. https://doi.org/10.1016/j.ecolind.2018.10.052.

Zhu, L., Song, R., Sun, S., Li, Y., Hu, K., 2022. Land use/land cover change and its impact on ecosystem carbon storage in coastal areas of China from 1980 to 2050. Ecol. Indic. 142, e109178 https://doi.org/10.1016/j.ecolind.2022.109178.